ACS APPLIED MATERIALS & INTERFACES

Applications of Polymer, Composite, and Coating Materials

Water-based PEDOT:Nafion Dispersion for Organic Bioelectronics

Stefano Carli, Michele Di Lauro, Michele Bianchi, mauro murgia, Anna De Salvo, Mirko Prato, Luciano Fadiga, and Fabio Biscarini

ACS Appl. Mater. Interfaces, **Just Accepted Manuscript** • DOI: 10.1021/acsami.0c06538 • Publication Date (Web): 09 Jun 2020

Water-based PEDOT:Nafion Dispersion for Organic Bioelectronics

Stefano Carli,† Michele Di Lauro,† Michele Bianchi,† Mauro Murgia,†|| Anna De Salvo,†§ Mirko Prato,‡ Luciano Fadiga,†§ Fabio Biscarini†⊥*

† *Center for Translational Neurophysiology, Istituto Italiano di Tecnologia 44121 Ferrara, Italy.*

|| *Istituto per lo Studio dei Materiali Nanostrutturati (ISMN) CNR, 40129 Bologna, Italy*

‡ *Materials Characterization Facility, Istituto Italiano di Tecnologia 16163 Genova, Italy*

§ *Section of Physiology, University of Ferrara 44121 Ferrara, Italy*

KEYWORDS. Conductive polymers, PEDOT, Nafion, PEDOT:Nafion, PEDOT:PSS, bioelectronics, drop casting, organic electrochemical transistors (OECTs).

ABSTRACT. The water dispersion of the conductive polymer poly(3,4-ethylenedioxythiophene):poly(styrenesulfonic acid) (PEDOT:PSS) is one of the most used material precursor in organic electronics also thanks to its industrial production. There is a growing interest for conductive polymers that could be alternative, surrogate or replace PEDOT:PSS in some applications. A recent study by our group compared electrodeposited PEDOT:Nafion vs PEDOT:PSS in the use for neural recordings. Here we introduce an easy and reproducible synthetic protocol to prepare a water dispersion of PEDOT:Nafion. The conductivity of the pristine material is on the order of 2 S cm^{-1} and was improved up to ≈6 S cm^{-1} upon treatment with ethylene glycol. Faster ion transfer was assessed by electrochemical impedance spectroscopy (EIS) and, interestingly, an improved adhesion was observed for coatings of the new PEDOT:Nafion on glass substrates, even without the addition of the silane cross-linker needed for PEDOT:PSS. As proof of concept, we demonstrate the use of this novel water dispersion of PEDOT:Nafion in three different organic electronic device architectures, namely an Organic Electrochemical Transistor (OECT), a memristor and an artificial synapse.

INTRODUCTION

Poly(3,4-ethylenedioxythiophene):poly(styrenesulfonic acid) (PEDOT:PSS) was chemically synthesized for the first time in 1988, as a stable water dispersion.[1] Since then, PEDOT:PSS has become perhaps the most important and most used conductive polymers in organic electronics.[2] Multiple factors contributed to the enormous growth of PEDOT:PSS market, including good film-forming properties, high transparency in the visible range, excellent thermal stability and high conductivity. The conductivity of the as-prepared PEDOT:PSS can be further improved by treatment with polar additives, surfactants, salts and acids.[3] For instance, the conductivity of the commercially available Clevios PH1000, which represents one of the highly conductive forms of commercial PEDOT:PSS dispersions, can be increased from approximately 1 S cm^{-1} up to 1000 S cm^{-1}.[3] Conductive polymers can be obtained either through electrochemical and chemical pathways. The big advantage of the chemical synthesis relates to the fact that it is well suited for industrial scale up. On the other hand, the electrochemical polymerization is particularly useful for those applications that require, for example, a

strict control of the deposited film in terms of electroactive area, thickness or doping content.[4,5] Formulations of PEDOT:PSS are often used for organic electrochemical transistor (OECT) and, in general, for bioelectronics.[6] Nevertheless, an increasing number of researchers have recently directed their efforts towards developing alternative materials to the commercially available PEDOT:PSS water dispersions. Among these, Tekoglu and co-workers have prepared a PEDOT- deoxyribonucleic acid (DNA) biocomposite that may embody specific biorecognition properties.[7] Other studies are aimed to replace PSS with biomolecules suitable for improving the biocompatibility of the blend, or to develop a drug delivery material, either for chemically or electrochemically prepared PEDOT.[8–10] Still, the incorporation of the sterically hindered PSS in PEDOT was found to be disadvantageous in DSSCs suggesting that the high conductance is not the only appealing requirement in organic electronics.[11] Nafion is the best-known ionomer membrane behaving as a solid, proton conducting electrolyte in electrochemical technology. The molecular structure of Nafion is characterized by a hydrophobic polytetrafluoroethylene backbone with regularly spaced shorter perfluorovinyl ether side-chains, each terminated by a strongly hydrophilic sulfonic acid

group (see Figure 1 and S1).[12] The greatest interest in Nafion in recent years arises from its potential role as a proton conducting membrane in fuel cells. Indeed, a proton conductivity on the order of 0.09 S cm^{-1} has been reported for Nafion 117 membranes, together with a specific capacitance of 64 nF g^{-1}.[13] Chemical polymerization of pyrrole and 3,4-ethylenedioxythiophene (EDOT) on Nafion 117 membranes was reported in the literature.[14] Recently the group of Christian Müller fabricated melt-spun PEDOT:Nafion fibers through the polymerization of PEDOT within a Nafion template. They also provided the performance of PEDOT:Nafion as a mixed ion-hole conductor in OECTs.[15] Our group reported electrodeposited PEDOT:Nafion on neural microelectrodes to yield higher charge injection limit when compared to the classic electrodeposited PEDOT:PSS, which makes it a good candidate for both neural recording and stimulation.[16] Advantages of electrodeposited PEDOT:Nafion for neurotransmitters detection have been described recently in the literature.[17,18] Nevertheless, the synthesis of a highly conductive water dispersed PEDOT:Nafion composite, that could indeed be compared to the existing water-based formulations of PEDOT:PSS, has never been reported to date. To the best of our knowledge, only three examples in the literature

reported on the chemical polymerization of EDOT in the presence of Nafion, although leading to poorly conductive materials (<<0.001 S cm^{-1}) thereby failing to attract the attention of the organic electronics community.[19,20]

The present work is aimed to provide an easy and efficient protocol to prepare a water dispersion of PEDOT:Nafion as a functional alternative to the well-known PEDOT:PSS in the field of organic electronics. The new PEDOT:Nafion water dispersion has been characterized by means of optical molecular and vibrational spectroscopy, X-ray photoelectron spectroscopy (XPS), cyclic voltammetry (CV), electrochemical impedance spectroscopy (EIS) and atomic force microscopy (AFM). Finally, the obtained PEDOT:Nafion has been used as active material in three different organic electronic devices as a proof-of-concept of its use in different applications: namely OECTs for bioelectronics, non-volatile memories (memristors) and artificial synapses. [21–23]

EXPERIMENTAL SECTION

Materials

Nafion dispersion (10 wt. % in H_2O, eq. wt. 1100), EDOT, anhydrous Iron(III) chloride ($FeCl_3$), 3-Glycidyloxypropyl)trimethoxysilane (GOPS), ethylene glycol (EG), and sodium chloride (NaCl) were purchased from Sigma Aldrich (Italy). Conductive fluorine tin oxide (FTO) glass (25/25/1.1 mm, 7-15 Ω sq^{-1}) was from Redoxme AB (Sweden). Ultrapure water (Milli-Q, Millipore, USA) was used for this study. PEDOT:PSS solution (Clevios PH1000) was purchased from Heraeus Precious Metals GmbH & Co. (Leverkusen, Germany). The nominal solid content and PEDOT to PSS ratio of the PH1000 solution are 1−1.3% and 1:2.5 by weight, respectively.

Synthesis of PEDOT:Nafion

The dispersion of Nafion (2 mL, 0.19 mmol) was diluted with water (6 mL) and EDOT (20μL, 26.62 mg, 0.187 mmol) was added. The mixture was vigorously stirred under a N_2 atmosphere for 30 minutes and EDOT was completely dissolved. $FeCl_3$ (60.75 mg,

0.374 mmol) was added and stirring was continued for 24 hours, at room temperature and under N_2. Water (10 mL) was added and the crude reaction mixture was centrifuged. The supernatant, which contains impurities and unreacted materials, is separated whereas the dark blue solid is re-dispersed in water (15 mL). This process is continued several time (typically 6-7 times), when the absorption spectrum of the supernatant presents no signals in the UV region (≈ 220-350 nm). Finally, the solid was dispersed in water (8 mL) to give a water dispersion of PEDOT:Nafion (density = 1.00 ± 0.01 g cm^{-3}). A reaction yield on the order of 50% is estimated, hinting that a 100% reaction yield should give a total amount of PEDOT comparable to the initial amount of EDOT.

Molecular and Vibrational spectroscopies

Absorption spectra were collected with a JASCO V 750 and V 570 UV–Vis spectrophotometers. Attenuated Total Reflection−Fourier Transform Infrared Spectroscopy (AT-FTIR) was performed with a FTIR spectrometer from JASCO (model

FT/IR 4600) equipped with a ATR accessory (ATR Pro One, JASCO). Analysis was collected on powder samples after removal of the solvent at room temperature.

Electrical and electrochemical characterization

The electrical conductivity was measured at room temperature by a standard four-probe method with a Reference 600 potentiostat (Gamry Instruments, USA) and a tester set in dc voltage mode. The van der Pauw method has been used to determine the electrical conductivity using the Gamry potentiostat as current source and measuring the correspondent voltage drop with a multimeter (Meterman 38XR).[24] Film thickness were measured with a KLA Tencor Stylus Profiler P7 profilometer.

CV and EIS were carried out using a Reference 600 potentiostat (Gamry Instruments, USA) connected to a three-electrode electrochemical cell with a large area Pt foil as a counter electrode and a Ag/3M AgCl reference electrode (+0.197 V vs NHE).[25] CV were collected at the scan rate of 50 mV s^{-1}. EIS were performed at 0 V by superimposing a voltage sine wave modulation (10 mV RMS amplitude) within the frequency range of 10^{5}–10^{-1} Hz. The software ZSimpWin V 3.2 (EChem Software) was used for equivalent

circuit modeling of EIS data and χ^2 values in the range of 10^{-4}–10^{-5} were used to estimate the covergence of the fit. The electrochemical characterizations were collected in saline (0.9% w/w NaCl aqueous solution). Samples were coated on FTO glass substrate by drop casting (30 µL) a previously diluted (1:6) dispersion of PEDOT:Nafion (N3, see Table 1) or PEDOT:PSS (PH1000). A small amount of GOPS (0.2 % volume) was added to PH1000 in order to improve the adhesion of the film.[26] The samples were dried at room temperature for 3 hours and baked at 100°C for 30 minutes.

Spectroelectrochemistry

Samples were coated on FTO glass substrate by drop casting and placed in a cuvette (Hellma, optical glass, spectral range 320-2500 nm, path length 10 mm, chamber volume 3,500 µL) containing saline installed in the beam path of the spectrophotometer. Spectroelectrochemistry data was recorded in a two electrode cell, using an Ag wire as the counter/reference electrode and the coated FTO electrode set as the working. Applied voltages for the Ag wire were rescaled vs. Ag/Ag^+ using $K_4[Fe(CN)_6]$ as a standard. The potentials in spectroelectrochemical studies were controlled using the

Gamry Reference 600 potentiostat and spectra were recorder while applying a constant cathodic potential at the working electrode.

Surface analysis

All films were prepared by drop casting the solution of PEDOT:Nafion or PH1000 on glass slices (10/20 mm). XPS measurements were conducted on a Kratos Axis Ultra DLD spectrometer, using a monochromatic Al Kα source (15 kV, 20 mA). Wide scans were acquired at an analyzer pass energy of 160 eV. High-resolution narrow scans were performed at a constant pass energy of 20 eV in 0.1 eV steps. Photoelectrons were detected at a takeoff angle Φ of 0° with respect to the surface normal. The pressure in the analysis chamber was kept below 6 × 10-9 Torr for data acquisition. The data were converted to VAMAS format and processed using CasaXPS version 2.3.19. The binding energy scale was internally referenced to the C 1s peak (BE for C−C of 284.8 eV).

SEM imaging was performed with a Zeiss EVO 40 electronic microscope with a maximum acceleration voltage of 20 KV. The sample were carbon coated with a ≈10 nm thick film.

AFM images were acquired in air at room temperature using a Park XE7 AFM System (Park Systems, Suwon, Korea) operated in tapping mode. Pre-mounted silicon cantilevers with backside reflecting coating (Al), typical tip curvature radius ~7 nm, k ~26 N/m and resonant frequency of ~300 kHz were used (OMCL-AC160TS, Olympus Micro Cantilevers, Tokyo, Japan). Average surface roughness from several random regions was expressed as RMS (Root Mean Square Roughness) ± standard deviation. The Height-Height Correlation Function, $H(r) = 2\sigma^2\,[1-e^{-(\frac{r}{\xi})^{2\alpha}}]$ was used to extract characteristic distance (r_c) values from 2 x2 μm^2 topography images; σ is the surface roughness, α is the Hurst parameter or roughness exponent, and ξ is the correlation length associated to a characteristic length scale in the image, such as average grain size or distance between two adjacent fibers.[27] The images were analyzed using

Gwyddion 2.55 Free SPM Software and Park Systems XEI Software (Park Systems, Suwon, Korea).

Device fabrication and characterization

Three different device architectures featuring PEDOT:Nafion as active material were demonstrated: OECT, memristor and artificial synapse. OECT and artificial synapse were fabricated depositing 0.5 µL of a 1:6 dilution of as-synthesized PEDOT:Nafion in MilliQ water on custom-designed test patterns (Phoenix S.R.L., Italy). Each test-pattern features nine independent pairs of gold Source/Drain electrodes (width-to-length ratio W/L=4) patterned onto a flexible polyimide substrate. Memristors were obtained casting 10 µL of the same PEDOT:Nafion formulation on photolithography/lift off made Au/quartz test-patterns (FBK, Trento, Italy) with W/L=10. Deposition was followed by three subsequent dipping steps (1 min in ethylene glycol, 30 s in ethanol and 30 s in MilliQ water) and by curing in thermostatic oven (120°C, 45min). A two-channel Source-Measure Unit (Keysight B2912A) was used to characterize device performances using Phosphate Buffer Solution (Sigma P3619-1GA, pH 7.4) as electrolyte and Pt foil as bath

electrode, the latter acting as gate in OECTs and memristors, and pre-synaptic terminal in artificial synapses.

Statistical Analysis

All experiments have been conducted at least in triplicate, except otherwise specified. Data were expressed as the mean ± standard deviation (SD) or standard error of the mean (SEM) where specified. Differences between groups were analyzed by a two sample Student's t-test. Significance was set at $p < 0.05$. All statistics were performed using the software OriginPro 2016 (OriginLab Corporation, MA).

RESULTS AND DISCUSSION

Synthesis

Oxidative polymerization of EDOT follows a path in which the starting point is the extraction of an electron from the monomer which forms radical cation intermediates. These radicals initiate the oligomer growth and, once the neutral form of PEDOT is obtained, the excess of charge corresponds to the reversible oxidation or doping level of

the polymer.[28] Both ammonium persulfate (APS) and $FeCl_3$ have been extensively used for the preparation of PEDOT:PSS or, in general, for the synthesis of PEDOT based water dispersions.[29] $FeCl_3$ is a milder oxidant (E^0 = 0.77 V Vs NHE), whereas the peroxydisulfate anion $S_2O_8^{2-}$, with a standard reduction potential of +2.01 V (Vs NHE), is one of the most powerful oxidants.[30] It is known that the solubility of EDOT in water is low, on the order of 2.1 g l^{-1} (10^{-2} M).[31] In our previous study, we have successfully electrodeposited PEDOT:Nafion films from a solution of 0.01 M EDOT in a mixture of Nafion and water.[16] In the present study we adopted similar conditions, in order to account for a complete dissolution of the monomer. We found that in similar conditions $FeCl_3$ provided better results than APS, in terms of improved conductivity and higher reproducibility, as reported in Table 1. We did not investigate the reasons of this behavior and $FeCl_3$ was the oxidant preferred in this study. Thus, an excess of $FeCl_3$ was added to the solution of EDOT in Nafion and the reaction mixture turns a deep blue color within 10-30 minutes. The appearance of polaron tails is confirmed by the increased absorbance at wavelengths higher than 500 nm. This indicates that the progression of the polymerization produces polarons and bipolarons charge carriers in

the new formed PEDOT:Nafion chains.[32] Thus, the reaction can be easily monitored through UV-Vis spectroscopy by observing the variation of the spectra over time. [33] In Figure S2 we present the typical spectral evolution during the oxidative polymerization of EDOT in the presence of Nafion and $FeCl_3$. A sketch of the reaction is reported in Figure 1.

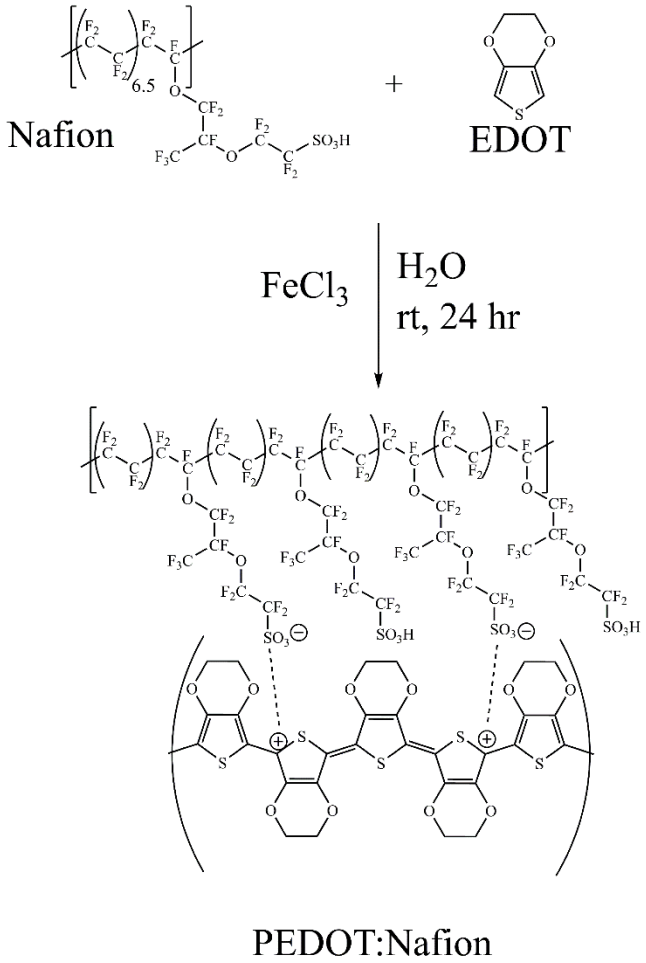

Figure 1. Synthetic route to PEDOT:Nafion water dispersion.

The conductivities of the most promising PEDOT:Nafion composites, obtained at different [Nafion] to [EDOT] molar ratios, are in the range of 0.3-2 S cm^{-1}, as reported in Table 1. In accordance with Zotti *et al.*, the sulfonate to thiophene molar ratio $R_{S/T}$ for the various PEDOT:Nafion samples were determined by XPS analysis.[34] We then related the conductivity of the obtained PEDOT:Nafion dispersions with their respective $R_{S/T}$ ratios. In the same conditions PH1000 exhibited a conductivity of 0.54 S cm^{-1} ± 0.03, in accordance with the literature.[35] Moreover, the conductivity of PEDOT:PSS prepared with $FeCl_3$, following a procedure similar to our study, was reported on the order of 10^{-1} S cm^{-1}.[36]

Table 1. Conductivity of PEDOT:Nafion

Sample ID	[Nafion]/[EDOT]	σ (S cm^{-1})	$R_{S/T}$[a]
N1	2.44	0.36 ± 0.04	7.0 ± 0.6
N2	1.22	1.5 ± 0.2	2.8 ± 0.1
N3	1.01	2.0 ± 0.3	2.3 ± 0.1

N4	0.81	1.9 ± 0.4	1.6 ± 0.2
N1A[b]	2.44	<<0.01	5.9 ± 0.1
N2A[b]	1.22	0.05 ± 0.006	1.5 ± 0.6
N4A[b]	0.81	0.37 ± 0.03	1.6 ± 0.3

[a] by XPS analysis; [b]oxidant: APS 1.01 eq. molar, 24 hr, room temperature.

It should be noticed that the conductivity of PEDOT:PSS is strongly influenced by the ratio between PSS and PEDOT. In general, lower conductivities are observed when an excess of the insulating PSS is incorporated within PEDOT:PSS.[34] Interestingly, we found a strong correlation between [Nafion]/[EDOT] and the resulting $R_{S/T}$ parameter, which decreases as the amount of EDOT is increased, with respect to Nafion. A significant improvement of the conductivity of PEDOT:Nafion can be observed when [Nafion]/[EDOT] is reduced from 2.44 to 1.22, reflecting a $R_{S/T}$ parameter of 7 and 2.8, respectively. Further reduction of $R_{S/T}$, yielded the highest conductivity on the order of 2 S cm^{-1} when the ratio between Nafion and EDOT is maintained at about 1-0.8. Notably,

it was observed that a reduction of the [Nafion]/[EDOT] value below 1 (sample N4, Table 1) leads to the formation of aggregates, suggesting that the solubility of PEDOT:Nafion in water and/or its deposition becomes problematics. This can be outlined in Figure S3, which present the SEM images of N3 and N4 films on glass substrates. Coating of N3 (S3a) is homogenous while the N4 (S3b) film is more irregular with evident aggregation, big cracks and exposed glass areas. Thus, albeit N3 and N4 exhibit comparable highest conductance, N3 is the best candidate to be used in organic electronics and, from this point onward, the abbreviation PEDOT:Nafion will refer to the sample N3. A notorious disadvantage of PEDOT:PSS coatings is related to the poor adhesion to the substrates when exposed to water. In other words, PEDOT:PSS films show a tendency to delaminate. A common solution to this problem is represented by the addiction of an epoxy-silane, the well-known GOPS, to PEDOT:PSS dispersion in order to increase the mechanical adhesion of the films. This approach improves significantly the robustness of the film, thereby avoiding delamination, but it negatively affects the conductivity of the resulting conductive films, when compared to the untreated PEDOT:PSS. Fabiano et al. suggested a possible mechanism to explain the

nature of the reduction of conductivity in PEDOT:PSS treated with GOPS. It is known that alkoxysilanes give cross-linkages through siloxanes formation, but they also demonstrated the formation of a covalent bond between the sulfonate groups of PSS chains and the epoxide moieties of GOPS, which is the cause of the conductivity reduction.[35] Thus, reducing the amount of GOPS or eliminating it may result extremely beneficial for future applications in organic electronics. Surprisingly, we found that PEDOT:Nafion coatings did not delaminate under the same conditions even without the addiction of GOPS. To prove that, we have monitored the absorbance of PEDOT:Nafion coatings on glass substrates over a period of 30 days immersed in water. Indeed, UV analysis confirmed no significant film detachment in this period of time in water (see Figure S4). Interestingly, it has been reported that films on glass of Nafion 117 were quickly and quantitatively removed from the surface when rinsed in water.[37] Our results indicate a synergistic effect between PEDOT and Nafion in the new composite PEDOT:Nafion composite in improving surface adhesion when compared to both pristine Nafion or PEDOT:PSS.

Electronic and Vibrational spectroscopies

In Figure 2a the presence of a broad band of absorption over the Visible-near infrared region (Vis-NIR) accounts for the formation of highly doped PEDOT.[38] It is known that PEDOT exhibits different doped states, but only polaron and bipolaron are poorly or highly conductive, respectively, whereas the neutral form is not conductive.[32] Thus, the strong absorption tail in the NIR region and the high optical transparency in the Vis region, both account for a highly doped bipolaron state of PEDOT:Nafion.[28] The comparison between the UV-Vis spectra of N1-4 samples (Figure S5) indicates that there are no significant differences in terms of their electronic transitions. This further corroborates the hypothesis that the conductivity is strongly influenced by the $R_{S/T}$ parameter. Figure 2b compares the FT-IR spectra of Nafion and PEDOT:Nafion. The spectrum of Nafion is dominated by the strong signals at 1200 cm^{-1} and 1142 cm^{-1} which relate to the coincidence of the asymmetric stretching of CF_2 and SO_3H, and the very intense band of the CF_2 asymmetric stretching mode, respectively.[39] The absorption band of medium intensity at 1054 cm^{-1}

has been assigned to the symmetric stretching of the sulfonic groups.[39] A blue-shift of the sulfonate groups peak(from 1054 cm^{-1} to 1065 cm^{-1}) is consistent with a change in the coordination pool of the sulfonic groups, likely due to the electrostatic interaction between SO_3^- and the positively charged PEDOT chains. Additionally, a significant downward shift (on the order of ≈25 cm^{-1}) of the CF_2 vibrations can be observed in the region of 1100-1200 cm^{-1}, if compared to pure Nafion. A similar effect was reported by Tsai and co-workers for Nafion™ membranes when immersed in water for a long time. Authors suggested that this effect is due to the interaction of water with both the hydrophilic and the hydrophobic domains of Nafion.[40] In Figure S6 we report a comparison between FT-IR of PEDOT:Nafion and PH1000. The inclusion of PEDOT in Nafion generates the appearance of the broad band centered at ≈1300 and ≈1500 cm^{-1} which accounts for C-C and C=C stretching modes for thiophene ring of PEDOT backbone.[41] Interestingly, the vibration mode at ≈1500 cm^{-1} , which was assigned to the quinoidal form of EDOT, is slightly up-shifted for PH1000 if compared to PEDOT:Nafion (see Figure S6). Vibration at 1000 cm^{-1} can be assigned to the stretching mode in the C-O-C bond of ethylenedioxy

residues of PEDOT, whereas further signals at ≈680 cm^{-1} and 860 cm^{-1} originate from the C-S bond vibration of the thiophene ring.[42]

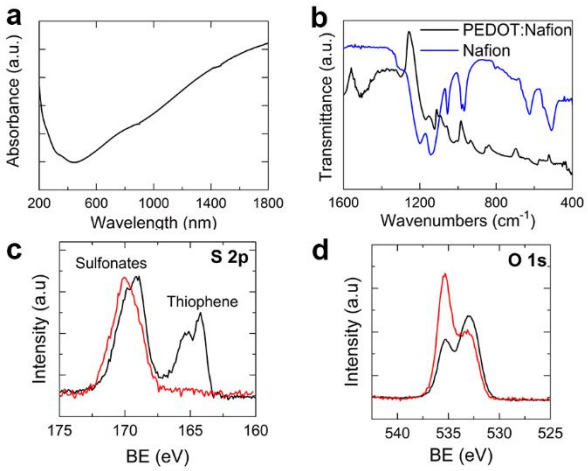

Figure 2. a) UV-Vis-NIR Absorption spectra of PEDOT:Nafion. b) FT-IR spectra of PEDOT:Nafion and Nafion. c) S (2p) and d) O (1s) core-level spectra, of PEDOT:Nafion (black line) and Nafion (red line).

XPS analysis

Surface chemical analysis of PEDOT:Nafion was performed by means of XPS analysis (Table S1).[43] Figure S7 compares the wide scan analysis of N3 and N4a (see

Table 1), and it can be seen that, in both cases, the spectra are dominated by the signals of sulfur, carbon, oxygen and fluorine. In Figure 2c the S 2p profile obtained from PEDOT:Nafion is characterized by the presence of two distinct sulfur species that can be ascribed to the sulfonate groups of Nafion (broad peak centered at approx. 169.4 eV) and to the sulfur atoms of the thiophene moiety in the PEDOT (doublet of peaks at lower binding energy of approx. 164 eV and 165 eV).[44,45] The band of SO_3H groups in pure Nafion is located at the higher binding energy (BE) of ≈170 eV, which indicates a higher electronic density around the sulfonic acid groups in PEDOT:Nafion. Interestingly, the sulfonate signals of PH1000 are located at the lower binding energy of 168.6 eV (Figure S8a). It is known that the binding energy of sulfonate groups in PSS is affected by the electronic density around the sulfur nucleus.[43] Thus, results here are consistent with a lower charge density around sulfonates groups in PEDOT:Nafion when compared to PH1000. This can be explained taking into account the very strong electron-withdrawing character of the fluorocarbon chains in Nafion, thereby leading to a pK_a which was estimated on the order of -3, whereas for PSS a higher value of pK_a ≈1.2 was reported.[46,47] The O 1s spectrum of Nafion (Figure 2d) contains two main

components, the stronger at the higher binding energy of 535.4 eV and the minor at 533.1 eV coming from the etheric and sulfonic groups, respectively.[48] These signals are observed also for PEDOT:Nafion but, in this case, the oxygens in the dioxyethylene bridge of PEDOT produce an increase of the intensity of the peak at the binding energy of ≈533 eV.[49] Interestingly, the signals related to dioxyethylene oxygen atoms are downshifted of about 0.8 eV in PH1000, as reported in Figure S8b. The C 1s spectrum of Nafion shown in Figure S8c has two main peaks at 291.6 eV (strong) and at 293.2 eV (shoulder). The lower binding energy signal is generated by the CF_2, whereas the smaller component has been assigned to CF_3.[48] Other low intensity peaks are present at approx. 290 eV (due to –OCF2– groups) and 287 eV (assigned to CF groups). When PEDOT is incorporated in Nafion to give PEDOT:Nafion, the new peaks relative to C-C/C-H, C-S, C=C-O, and C-O-C groups of PEDOT are also observed in the energy range of 285-287 eV.[49] Elemental composition of PEDOT:Nafion samples and Nafion, as calculated from XPS analysis, are reported in Table S1. The repeating unit in Nafion ($Nafion_{monomer}$) has the generic formula $C_{20}HF_{39}O_5S$ (Figure S1) thus, a theoretical fluorine-to-sulfur molar ratio ($R_{F/S}$) of 39 should be expected for Nafion. Nevertheless, a

higher value of $R_{F/S}$ on the order of 70 was obtained *via* XPS for Nafion, which is consistent with a higher abundance of fluorine atoms. This effect was ascribed to a displacement of the sulfonic acid groups away from the surface, as reported by other authors.[50] Indeed, according to Gierke model, the structure of Nafion is dominated by the presence of inverted micelles, where the polymeric ions and absorbed water separate from the fluorocarbon matrix into approximately spherical domains connected by short narrow channels.[51] Given that $R_{S/T}$ provides the molar ratio between monomeric units of Nafion and EDOT units in PEDOT:Nafion, theoretical values of $R_{F/S}$ for N1-N4 samples can be calculated according to the stoichiometry of the repeating unit of PEDOT:Nafion, which can be expressed as $[R_{S/T}(Nafion_{monomer})][EDOT]$ (see Table S1). Interestingly, the introduction of PEDOT in Nafion produces a significant reduction of the $R_{F/S}$ ratio for all PEDOT:Nafion samples (N1-N4) toward the expected theoretical value, and this effect is more pronounced as the amount of PEDOT increases (see Table S1). Thus, the higher concentration of sulfonic acid groups on the surface of PEDOT:Nafion (N1-N4), in comparison to pristine Nafion, suggests that the incorporation of PEDOT brings the (buried) hydrophilic domains of Nafion on the surface.

Electrochemistry and Spectro-Electrochemistry

Conjugation length and conjugation defects along the polymer backbone play an important role to determine the overall conductivity. Indeed, the electrical conductivity of PEDOT can be improved by tuning the conjugation length and/or increasing the doping level.[52] In general, an extended conjugation length of PEDOT reduces the HOMO-LUMO energy bandgap of the neutral state, thereby shifting the π-π^* transition to lower energies. Thus, spectro-electrochemical analysis was conducted in order to shed light on the relationship between the molecular structure of PEDOT:Nafion and its conductivity. Given that the absorption of the reduced form of PEDOT:PSS is typically centered at ≈630 nm, a negative shift of this maximum is likely due to the presence of shorter PEDOT chains.[53] As reported in Figure 3a the fully reduced form of PEDOT:Nafion exhibited a broad band centered at ≈620 nm. The spectrum of reduced PH1000 (Figure S9) outlines the presence of two maximum peaks at 637 nm and 690

nm, due to the presence of inequivalent quinoid and benzoid forms.[54] Thus, neutral PEDOT:Nafion exhibits a slight hypsochromic shift of the absorption maximum, if compared to PH1000, presumably due to a reduction of the conjugation length. Nevertheless, the extent of the conjugation length reduction does not seem to negatively affect the conductivity of PEDOT:Nafion, which is comparable to pristine PH1000 (see Table 1).[26,35] The CV trace of PEDOT:Nafion (Figure 3b) shows a capacitive behavior at positive voltages, and a strong faradaic activity at negative potentials, which is related to the reduction and re-oxidation of the PEDOT chains.[38] The main faradaic process of PEDOT:Nafion is centered at $E_{1/2}$ = -0.2 V and a peak separation ΔE = 240 mV. Another reduction peak can be identified at the lower potential of -0.7 V with a shoulder at -0.5 V, on the reverse scan.

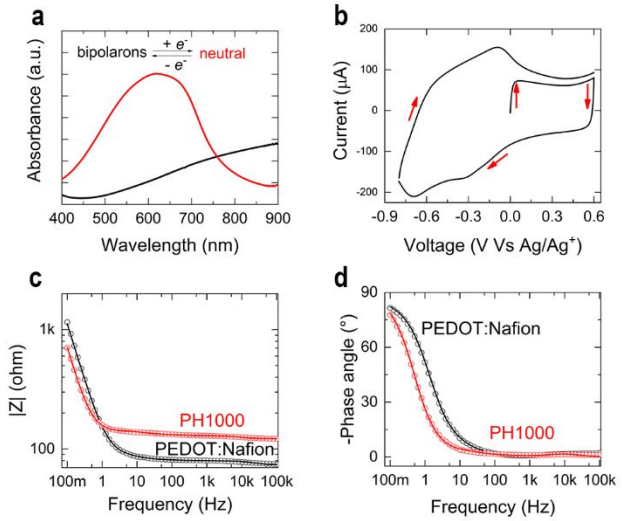

Figure 3. a) Spectroelectrochemistry of PEDOT:Nafion; b) CV of PEDOT:Nafion on FTO; representative fitting of experimental EIS data showing c) the Bode modules and d) the Bode phase angle plots (experimental data are reported as circles and theoretical data are presented as lines).

It was reported that the redox potential of PEDOT:PSS changes upon treatment with polar solvents, including EG. Authors suggested that the changes in redox behavior can be ascribed to the EG effect on PEDOT conformation.[55] Thus, our hypothesis is that two conformational domain can be present in PEDOT:Nafion films. In the case of PH1000 (Figure S10) the cathodic sweep exhibits a dominant process centered at -0.3 V (peak separation ΔE = 220 mV), in accordance with the literature.[56] Notably, both

PEDOT:Nafion and PH1000 exhibited a peak separation larger than 200 mV, thereby suggesting a slow kinetic process, as a consequence of in/out ions diffusion limitation. Indeed, the exact location of these redox signals was found to be strongly dependent not only on the nature of the dopant, but also on structural and morphological modification of the conductive film.[55,57] Taking into account the extremely low pKa of the sulfonic acid groups of Nafion, it is likely that the higher reduction potential of PEDOT:Nafion is the result of several contribution including, but not limited to, the electrostatic interaction between negatively charged sulfonate groups and the positively charged PEDOT units. EIS was collected in order to compare charge transport dynamics of PEDOT:Nafion and PH1000. Circuit modelling was also applied to provide a quantitative analysis of experimental EIS data. One of the most widely accepted electric circuit to model experimental EIS of PEDOT consists of a solution resistance R_S in series with a fast charge transfer process (a charge transfer resistance R_{CT} in parallel with a charge transfer capacitance C_{CT}), a double layer capacitance C_{dl} and a finite length Warburg impedance T.[58] The charge transfer process accounts for ion transport at the polymer|electrolyte interface.[58] The Warburg element describes the diffusion of

ions through the pores of PEDOT, and its impedance can be obtained by the formula $Z_D = (\tau_D/C_D)\coth(j\omega\tau_D)^{1/2}/(j\omega\tau_D)^{1/2}$ where j is the imaginary unit ($j^2 = -1$), ω is the angular frequency ($\omega = 2\pi f$, where f is the frequency), τ_D is the diffusional time constant, C_D is the pseudocapacitance and R_D is the diffusional resistance, the two determing the device timescale $\tau_D = R_D C_D$.[59] We found a better approximation when a constant phase element CPE was adopted in place of a pure capacitor (see Figure S11 for a sketch of the circuit model).[16,60] A CPE is often used to model the capacitance of not-ideal electrode surfaces, due for instance to the presence of rough and/or porous coatings. The impedance of a CPE is given by $1/Z_{CPE} = Q_{CPE} = Q_0(j\omega)^n$ where Q_{CPE} is the admittance of the CPE and Q_0 represents the admittance at $\omega = 1$ rad s^{-1}.[59] The good agreement between experimental and calculated EIS can also be observed by visual inspection in the Bode |Z| and phase angle plots (see Figure 3c and 3d, respectively). The relevant parameters obtained by the fitting are reported in Table S2. Interestingly, faster ion transport is observed for PEDOT:Nafion which yielded similar charge transfer resistances, but lower time constant than PH1000. Additionally, the exponent n of the CPE is on the order of 0.94 for PEDOT:Nafion whereas it was found to be 1 for

PH1000, thereby reflecting the behavior of an ideal capacitor of the latter. This deviation can be due, for example, to a larger roughness for PEDOT:Nafion surface compared to PH1000. The diffusion of ions through PEDOT:Nafion pores is facilitated, with respect to PH1000, as indicated by the lower R_D exhibited by the former. Notably, this is also consistent with a higher ion conductivity of PEDOT:Nafion.[61] Faster diffusion of ions through PEDOT:Nafion pores is also supported by the lower τ_D on the order of 0.13 s, if compared to ≈0.44 s obtained for PH1000, in accordance with our previous study on electrodeposited PEDOT:Nafion Vs PEDOT:PSS.[16] A capacitance of 3.3 ± 0.6 mF cm^{-2} was obtained for PEDOT:Nafion, which was extracted at the low frequency limit of the imaginary part of the impedance, following the relationship $-Z_{imm} = 1/(2\pi f C_{dl})$ (where f = 0.1 Hz).[59] Thus, PEDOT:Nafion coatings are characterized by a slightly lower capacitance compared to PH1000, that exhibited a value on the order of 4.6 mF cm^{-2} (see Table S2). According to the adopted electric model, the total capacitance $C_{dl} = (1/_{CPE} + 1/C_D)^{-1}$ arises from in-series electronic capacitance CPE and diffusional capacitance C_D.[62] Although the physical meaning of the admittance Q_0 of the CPE can be ascribed to a pure capacitance only when ω = 1 rad s^{-1} or when n = 1, the lower Q_0

exhibited by PEDOT:Nafion is consistent with the smaller electronic capacitance with respect to PH1000.[62] It was reported that the electronic capacitance of PEDOT:PSS relates to the amount of charge carriers.[62] Thus, a possible explanation of the reduced capacitance of PEDOT:Nafion can be linked to a slightly lower amount of charge carriers in the water dispersion, compared to the solution of PH1000. According to the customer, the PEDOT:PSS content in the dispersion of PH1000 is in the range of 1-1.3 % by weight with a PSS to PEDOT ratio of 2.5. This corresponds to a PEDOT content on the order of 0.2-0.3 % by weight. A solid content of about 3.1-3.3 % was estimated for PEDOT:Nafion water dispersion thus, according to XPS analysis which provided a Nafion to PEDOT molar ratio of 2.2, this corresponds to a PEDOT content of ≈0.1-0.2 % by weight (see Table S3). To sum up, the reduced capacitance observed for PEDOT:Nafion can be ascribed to a slightly lower amount of PEDOT compared to PH1000.

AFM analysis

In Figure 4a-d we report the results of AFM investigation carried out on PEDOT:Nafion films deposited on FTO substrates. As prepared PEDOT:Nafion films exhibit a one-order-of-magnitude-higher surface roughness (RMS = 18 ± 3 nm, calculated on a 2 x 2 μm^2 scan size) compared to PH1000 (RMS = 2.3 ± 0.8 nm, see Table S4 and Figure S12a, b), thereby corroborating EIS modelling results. In addition, the surface of PEDOT:Nafion is composed by round-shaped nanograins with a mean lateral size of ≈25-30 nm (Figure 4b, c), sharply contrasting the typical structure of pristine PH1000, composed by nanograins and fibrillar structures with size on the order of 20 nm (Figure S12b, c).[26] The analysis of the phase image signal (Figure 4d) reveals a roughly homogenous distribution of the phase angle values, which hints the identification of separated PEDOT and counterion phase, as found for pristine PH1000 (Figure S12d) and also reported in the literature.[26] It is known that PEDOT:PSS undergoes a phase separation between conductive PEDOT and insulating PSS chains, respectively, upon treatment with polar solvents like ethylene glycol (EG). This produces a large increase of the conductivity of PEDOT:PSS.[55] In the case of PEDOT:Nafion, the

same protocols used for PEDOT:PSS were not able to yield such an effective improvement of the conductivity.

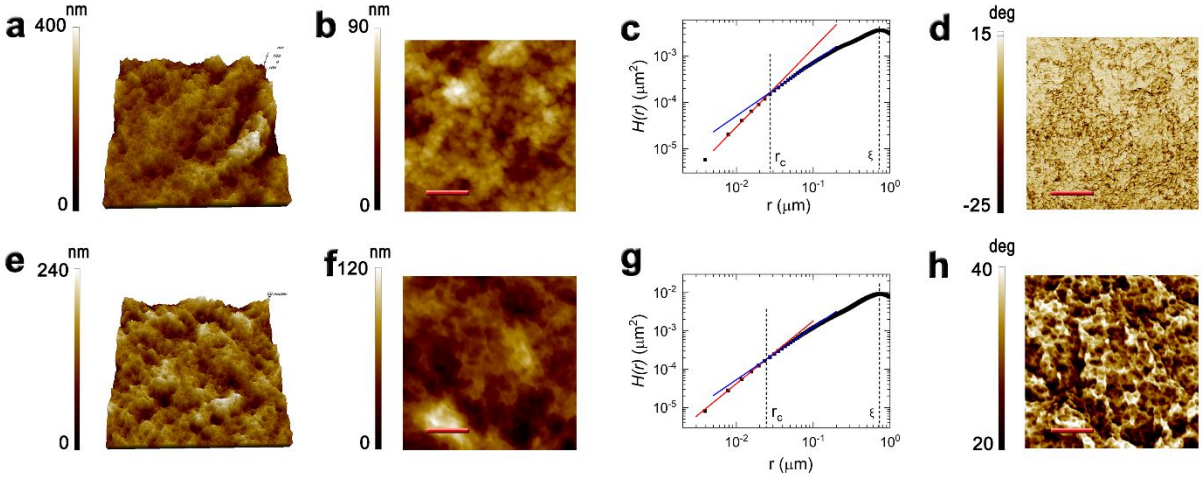

Figure 4. Results of AFM characterization carried out on PEDOT:Nafion (a-d) and PEDOT:Nafion+EG_{dip} (e-h) samples. a, e) 3D topographical rendering (scan size: 5 x 5 μm^2); b, f) 2D topography images (scan size: 1 x 1 μm^2, scale bar is 250 nm); c, g) Height-height Correlation Function plots in log-log scale: the characteristic distance r_c, can be obtained from the intercept of the power law fits of the two differently-scaling regimes in the self-affine regions of the HHCF plot (i.e. for $r < \xi$, the correlation lenght); d, h) phase images (scan size: 1 x 1 μm^2, scale bar is 250 nm).

The best results were obtained by dipping the coated films in EG and, subsequently in ethanol and water (see experimental) which yielded a conductivity of 5.5 ± 0.8 S cm^{-1}.

This protocol is similar to the one reported in the literature for PEDOT:PSS, which is known to have a significant effect on the final conductivity.[63] Indeed, the morphology of PEDOT:Nafion was markedly modified upon dipping in EG, as can be seen in Figure 4e and 4f. The most evident effect was the modification of the surface nanostructure, where the nano-size granular texture was replaced by a fibril-like structure, with fibrils of about 7-10 nm interconnected by pores of ~26 nm, (Figure 4g and Table S4). The phase signal (Figure 4h) appeared to follow the strong modification observed in the topography (Figure 4f). The fact that the phase signal well traced the topography signal, suggests that no distinct phases are segregated upon dipping PEDOT:Nafion in EG. More likely, the whole conductive polymer rearranged its structure into a fibrillary-like fashion. The absence of a clear phase segregation upon EG treatment may explain, at least in part, the modest improvement of the conductivity of PEDOT:Nafion if compared to PH1000 when treated in similar conditions.

Device Demonstration

Organic Electro-Chemical Transistor

PEDOT:Nafion-based OECTs have been characterized in the standard common Source-common Ground configuration. In this configuration, a PEDOT:Nafion film between two electrodes (namely the Source, *S*, and the Drain, *D*) acts as a semi-conductive channel, whose conductivity is modulated by the application of a voltage at a third electrode (the Gate, *G*). The Gate sets the potential of the electrolyte and, hence, the doping state of the conductive polymer (Figure 5a). As expected, due to the analogies with PEDOT:PSS, these devices work in depletion mode and to increase the channel resistance by more than an order of magnitude (ON/OFF ≈ 17) the Gate-to-Source voltage, V_{GS}, is scanned from -0.7V to 0.7 V at a fixed Drain-to-Source bias, V_{DS} = -0.7 V. The transfer characteristics are shown in Figure 5b. The derivative of this curve known as the transconductance g_m, is a direct measurement of the potentiometric sensitivity of OECT. Our PEDOT:Nafion OECTs exhibit g_m = 276 μS ± 15 μS, in line with common OECTs used for sensing and transduction, peaking at V_{GS} ≈ 100 mV.[64,65] In similar conditions PH1000 treated with polar low molecular weight additives (such as EG, DMSO, etc.) exhibits higher values of g_m, on the order of 1-10 mS. It is known that transconductance is directly related to hole mobility, which also directly relates to the

ohmic conductance of the conductive material.[66] Thus, the lower transconductance observed for PEDOT:Nafion can be rationalized referring to the already discussed modest improvement of its conductivity when treated in EG, if compared to PH1000. It is possible to observe a moderate counterclockwise hysteresis, which is in good agreement with the slower re-oxidation kinetics observed in CV analysis. Output characteristics of these devices (Figure 5c), obtained scanning V_{DS} from 0 V to -0.7 V, show ohmic behavior for low V_{DS}, followed by saturation plateaus and showing no sign of relevant contact resistance.

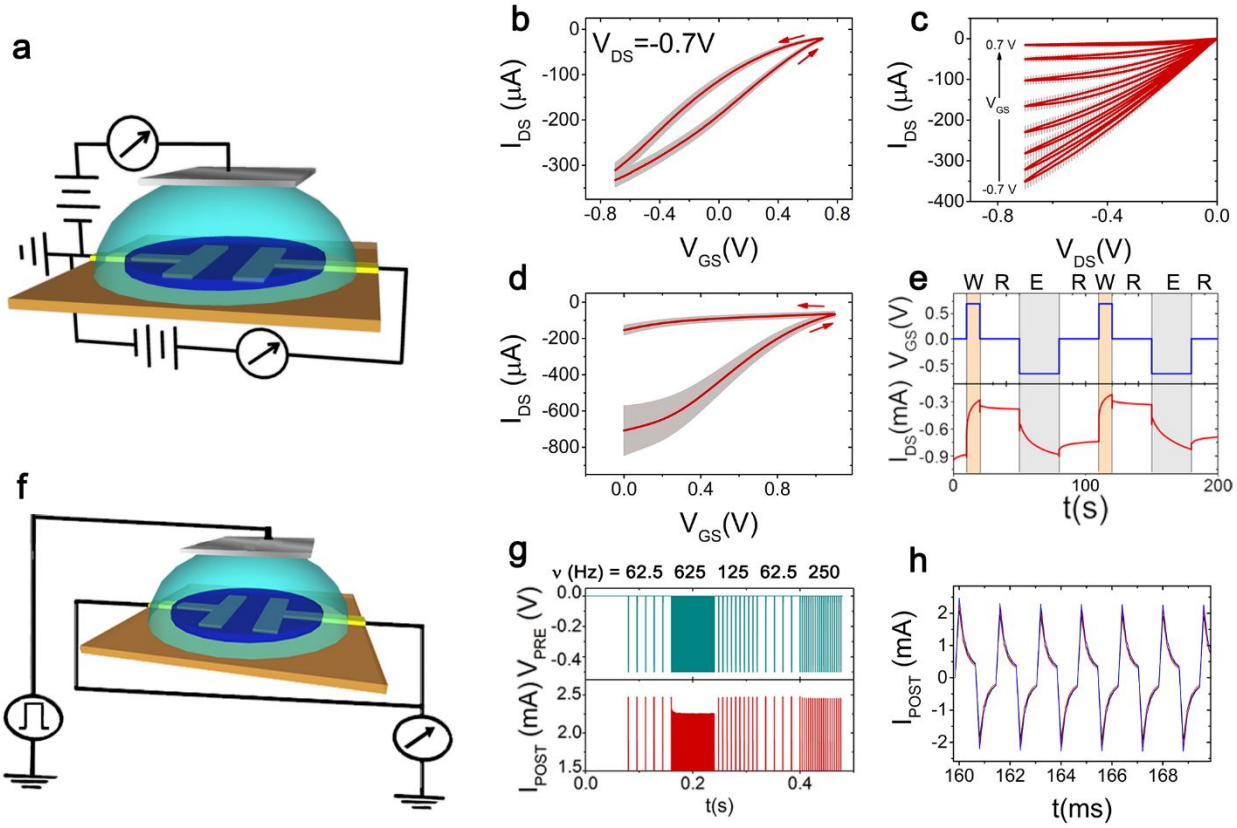

Figure 5. a) Connection layout for OECT and memristor devices; b-c) average transfer (b) and output (c) characteristics (n = 6) of PEDOT:Nafion OECTs reported with its SEM (grey area); d) average transfer characteristic of PEDOT:Nafion memristors (n = 7), reported with its SEM (grey area); e) voltammogram (solid blue line) and relative chronoamperometry (solid red line) showing resistive switching in memristors. Read, write and erase periods are highlighted in white, orange and grey, respectively; f) connection layout for pseudo-two-terminal artificial synapse; g) positive branch of the short-term plasticity neuromorphic response (I_{POST} vs t) in response to pulsed stimulation (V_{PRE} vs t); h) overlay of the depressive response (v = 625 Hz) of three different devices, the incomplete relaxation of the ions adsorbed/captured by PEDOT:Nafion gives rise to the depressive response.

Non-volatile memories (memristors)

The channel of an OECT can be tuned in order to obtain a non-volatile memory element whose resistance is shifted between two states by means of an electrochemical reaction.[22] In our PEDOT:Nafion OECTs this is achieved by simply increasing the thickness of the deposited PEDOT:Nafion layer and the geometrical factor W/L, where W and L are the channel width and length. Transfer characteristics of these devices, Figure 5d, exhibit lower channel resistance in the ON state and, subsequently, higher transconductances (g_m = 0.8 mS ± 0.2 mS), albeit with a positive shift of V_{GS} values necessary for de-doping and a more pronounced hysteresis. By exploiting the poor reversibility of the doping/de-doping processes in these architectures it is possible to obtain a low-power memory unit working in liquid (Figure 5e). When null V_{GS} is applied, the device is in the “read” condition and the current flowing in the channel upon the application of a V_{DS} depends on the doping state of the polymer. It is, hence, possible to switch it off (i.e. to “write”) by applying a positive V_{GS} and to turn it back on (i.e. “erase”) with a negative V_{GS}. The already discussed difference between the kinetics of doping

and de-doping implies longer times for erasing than those required for writing, allowing a stable memory effect. In the proposed protocol (10 s “writing”, 30 s “reading”, 30 s “erasing”, 30 s “reading”, etc.) it is possible to achieve a stable current difference between the written and erased states as high as 360 μA, in line with state of the art devices.[67] Analysis of the resistive switching behavior in Figure 5e suggests the possibility to achieve multiple memory states (i.e. channel resistance values) by properly tailoring writing and erasing times, thus technologically exploiting the aforementioned kynetic anisotropy of the dedoping/doping processes to obtain a non-binary memory element.

Artificial synapses

As already reported elsewhere, it is possible to operate liquid-gated organic electronic devices as pseudo-two-terminal neuromorphic devices exhibiting short-term plasticity (STP), with the connection layout depicted in Figure 5f.[23,68]

STP is one of the main functional features of biological synapses, consisting in the capability of facilitating or depressing the transmission of a stimulus from the pre-

synaptic neuron to the post-synaptic one, according to the stimulation frequency, resulting in dynamic time-dependent spike processing.[69] In these architectures, the potential of the "pre-synaptic" terminal, V_{PRE}, is pulsed with square waves at various frequencies while the resulting displacement current at the "post-synaptic" terminal, I_{POST}, is recorded. When the stimulation frequency is high enough, it is possible to mimic the depressive response of synapses, resulting in a I_{POST} decrease upon subsequent spiking, due to incomplete relaxation of the double layer, as shown in Figure 5h. When stimulation frequency is decreased, current response returns to linearity. In our PEDOT:Nafion-based artificial synapses it is possible to achieve 10% I_{POST} depression by stimulating at 625 Hz, with a characteristic depression timescale τ = 1.0 ms ± 0.1 ms, thus obtaining a novel organic frequency dependent switch operating in the kHz range.[70]

CONCLUSIONS

In conclusion, a facile synthetic route to obtain a water dispersed highly conductive PEDOT:Nafion composite was described. The relevant properties of the novel

PEDOT:Nafion have been assessed by physicochemical standard techniques and in organic electronic device architectures. Despite there is still room for future investigations aimed at increasing the conductance of pristine PEDOT:Nafion films, fast ion transport and stability to delamination, even in the absence of adhesion promoters, make PEDOT:Nafion a useful multifunctional material in the realm of printable organic electronics. Furthermore, we believe that the incorporation of Nafion in a conductive matrix like PEDOT:Nafion will be particularly promising in the field of bio-sensing. Indeed, Nafion is one of the most effective ion transporter and is extremely selective towards cations thus, we believe that the incorporation of Nafion in a conductive matrix like PEDOT:Nafion will be particularly promising in the field of bio-sensing and bioelectronics in vivo.

ASSOCIATED CONTENT

Supporting Information. The Supporting Information is available free of charge via the Internet at http://pubs.acs.org. Chemical formula of Nafion, UV-Vis spectra, spectroelectrochemistry, EIS, XPS, AFM.

AUTHOR INFORMATION

Corresponding Author

Stefano Carli, Center for Translational Neurophysiology, Istituto Italiano di Tecnologia, 44123 Ferrara (Italy). https://orcid.org/0000-0002-0309-2356

Email: stefano.carli@iit.it

Author Contributions

The manuscript was written through contributions of all authors. All authors have given approval to the final version of the manuscript.

REFERENCES

(1) Friedrich, J.; Kirchmeyer, S. Patent. 3813589, 1988.

(2) Lövenich, W. PEDOT-Properties and Applications. *Polym. Sci. - Ser. C* **2014**, *56* (1), 135–143. https://doi.org/10.1134/S1811238214010068.

(3) Shi, H.; Liu, C.; Jiang, Q.; Xu, J. Effective Approaches to Improve the Electrical Conductivity of PEDOT:PSS: A Review. *Adv. Electron. Mater.* **2015**, *1* (4), 1–16. https://doi.org/10.1002/aelm.201500017.

(4) Carli, S.; Casarin, L.; Bergamini, G.; Caramori, S.; Bignozzi, C. A. Conductive PEDOT Covalently Bound to Transparent FTO Electrodes. *J. Phys. Chem. C* **2014**, *118* (30), 16782–16790. https://doi.org/10.1021/jp412758g.

(5) Park, B. W.; Pazoki, M.; Aitola, K.; Jeong, S.; Johansson, E. M. J.; Hagfeldt, A.; Boschloo, G. Understanding Interfacial Charge Transfer between Metallic PEDOT Counter Electrodes and a Cobalt Redox Shuttle in Dye-Sensitized Solar Cells. *ACS*

Appl. Mater. Interfaces **2014**, *6* (3), 2074–2079. https://doi.org/10.1021/am405108d.

(6) Inal, S.; Rivnay, J.; Suiu, A. O.; Malliaras, G. G.; McCulloch, I. Conjugated Polymers in Bioelectronics. *Acc. Chem. Res.* **2018**, *51* (6), 1368–1376. https://doi.org/10.1021/acs.accounts.7b00624.

(7) Tekoglu, S.; Wielend, D.; Scharber, M. C.; Sariciftci, N. S.; Yumusak, C. Conducting Polymer-Based Biocomposites Using Deoxyribonucleic Acid (DNA) as Counterion. *Adv. Mater. Technol.* **2019**, *5* (3), 1900699. https://doi.org/10.1002/admt.201900699.

(8) Mantione, D.; del Agua, I.; Sanchez-Sanchez, A.; Mecerreyes, D. Poly(3,4-Ethylenedioxythiophene) (PEDOT) Derivatives: Innovative Conductive Polymers for Bioelectronics. *Polymers (Basel).* **2017**, *9* (8), 354. https://doi.org/10.3390/polym9080354.

(9) Carli, S.; Castagnola, E.; Vomero, M.; Scarpellini, A.; Prato, M.; Goshi, N.; Fadiga,

L.; Ricci, D.; Kassegne, S. Multilayer Poly(3,4-Ethylenedioxythiophene)-Dexamethasone and Poly(3,4-Ethylenedioxythiophene)-Polystyrene Sulfonate-Carbon Nanotubes Coatings on Glassy Carbon Microelectrode Arrays for Controlled Drug Release. *Biointerphases* **2017**, *12* (3), 031002. https://doi.org/10.1116/1.4993140.

(10) Carli, S.; Fioravanti, G.; Armirotti, A.; Ciarpella, F.; Prato, M.; Ottonello, G.; Salerno, M.; Scarpellini, A.; Perrone, D.; Marchesi, E.; Ricci, D.; Fadiga, L. A New Drug Delivery System Based on Tauroursodeoxycholic Acid and PEDOT. *Chem. - A Eur. J.* **2019**, *25* (9), 2322–2329. https://doi.org/10.1002/chem.201805285.

(11) Carli, S.; Busatto, E.; Caramori, S.; Boaretto, R.; Argazzi, R.; Timpson, C. J.; Bignozzi, C. A. Comparative Evaluation of Catalytic Counter Electrodes for Co(III)/(II) Electron Shuttles in Regenerative Photoelectrochemical Cells. *J. Phys. Chem. C* **2013**, *117* (10), 5142–5153. https://doi.org/10.1021/jp312066n.

(12) Mauritz, K. A.; Moore, R. B. State of Understanding of Nafion. *Chem. Rev.* **2004**, *104* (10), 4535–4585. https://doi.org/10.1021/cr0207123.

(13) Yadav, R.; Fedkiw, P. S. Analysis of EIS Technique and Nafion 117 Conductivity as a Function of Temperature and Relative Humidity. *J. Electrochem. Soc.* **2012**, *159* (3), 340–346. https://doi.org/10.1149/2.104203jes.

(14) Li, L.; Drillet, J. F.; Dittmeyer, R.; Jüttner, K. Formation and Characterization of PEDOT-Modified Nafion 117 Membranes. *J. Solid State Electrochem.* **2006**, *10* (9), 708–713. https://doi.org/10.1007/s10008-006-0115-1.

(15) Hofmann, A. I.; Ida, O.; Kim, Y.; Fauth, S.; Craighero, M.; Yoon, M.; Lund, A.; Mu, C. All-Polymer Conducting Fibers and 3D Prints via Melt Processing and Templated Polymerization. *ACS Appl. Mater. interfacesApplied Mater. interfaces* **2020**, *12* (7), 8713–8721. https://doi.org/10.1021/acsami.9b20615.

(16) Carli, S.; Bianchi, M.; Zucchini, E.; Di Lauro, M.; Prato, M.; Murgia, M.; Fadiga, L.; Biscarini, F. Electrodeposited PEDOT:Nafion Composite for Neural Recording and Stimulation. *Adv. Healthc. Mater.* **2019**, *8* (19), 1900765. https://doi.org/10.1002/adhm.201900765.

(17) Vreeland, R. F.; Atcherley, C. W.; Russell, W. S.; Xie, J. Y.; Lu, D.; Laude, N. D.; Porreca, F.; Heien, M. L. Biocompatible PEDOT:Nafion Composite Electrode Coatings for Selective Detection of Neurotransmitters in Vivo. *Anal. Chem.* **2015**, *87* (5), 2600–2607. https://doi.org/10.1021/ac502165f.

(18) Demuru, S.; Deligianni, H. Surface PEDOT:Nafion Coatings for Enhanced Dopamine, Serotonin and Adenosine Sensing. *J. Electrochem. Soc.* **2017**, *164* (14), G129–G138. https://doi.org/10.1149/2.1461714jes.

(19) Shiying, Z.; Steffen, Z.; Gang Chris, H.-A. Electrically Conductive Films Formed From Dispersions Comprising Polythiophenes and Ether Containing Polymers. US 2010/0081007 A1, 2010.

(20) HSU, C.-H.; Anders Paul Fahlman, M.; Slawomir Jacek, M.; Salaneck, W. R. Water Dispersible Polythiophenes Made with Polymeric Acid Colloids. US 7,390,438 B2, 2008.

(21) Bernards, D. A.; Malliaras, G. G. Steady-State and Transient Behavior of Organic

Electrochemical Transistors. *Adv. Funct. Mater.* **2007**, *17* (17), 3538–3544. https://doi.org/10.1002/adfm.200601239.

(22) Erokhin, V. Organic Memristors : Basic Principles. *Proc. 2010 IEEE Int. Symp. Circuits Syst.* **2010**, 5–8. https://doi.org/10.1109/ISCAS.2010.5537145.

(23) Giordani, M.; Berto, M.; Di Lauro, M.; Bortolotti, C. A.; Zoli, M.; Biscarini, F. Specific Dopamine Sensing Based on Short-Term Plasticity Behavior of a Whole Organic Artificial Synapse. *ACS Sensors* **2017**, *2* (12), 1756–1760. https://doi.org/10.1021/acssensors.7b00542.

(24) Pauw, L. J. van der. A Method of Measuring Specific Resistivity and Hall Effect of Discs of Arbitrary Shapes. *Philips Res. Rep.* **1958**, *13* (1), 1–9.

(25) Bard, A. J.; Faulkner., L. R. *Fundamentals and Applications Fundamentals and Applications*; J. Wiley & Sons: Hoboken, NJ, 2002.

(26) Crispin, X.; Jakobsson, F. L. E.; Crispin, A.; Grim, P. C. M.; Andersson, P.; Volodin, A.; Van Haesendonck, C.; Van Der Auweraer, M.; Salaneck, W. R.; Berggren, M.

The Origin of the High Conductivity of Poly(3,4-Ethylenedioxythiophene)-Poly(Styrenesulfonate) (PEDOT-PSS) Plastic Electrodes. *Chem. Mater.* **2006**, *18* (18), 4354–4360. https://doi.org/10.1021/cm061032+.

(27) Gambardella, A.; Berni, M.; Russo, A.; Bianchi, M. A Comparative Study of the Growth Dynamics of Zirconia Thin Films Deposited by Ionized Jet Deposition onto Different Substrates. *Surf. Coatings Technol.* **2018**, *337* (15 March), 306–312. https://doi.org/10.1016/J.SURFCOAT.2018.01.026.

(28) Roncali, J. Conjugated Poly(Thiophenes): Synthesis, Functionalization, and Applications. *Chem. Rev.* **1992**, *2* (4), 711–738. https://doi.org/10.1021/cr00012a009.

(29) Groenendaal, B. L.; Jonas, F.; Freitag, D.; Pielartzik, H.; Reynolds, J. R. Poly(3,4-Ethylenedioxythiophene) and Its Derivatives : Past , Present , and Future. *Adv. Mater.* **2000**, *12* (7), 481–494. https://doi.org/10.1002/(SICI)1521-4095(200004)12:7<481::AID-ADMA481>3.0.CO;2-C.

(30) Minisci, F.; Citterio, A.; Giordano, C. Electron-Transfer Processes: Peroxydisulfate, a Useful and Versatile Reagent in Organic Chemistry. *Acc. Chem. Res.* **1983**, *16* (1), 27–32. https://doi.org/10.1021/ar00085a005.

(31) Kudoh, Y.; Akami, K.; Matsuya, Y. Chemical Polymerization of 3,4-Ethylenedioxythiophene Using an Aqueous Medium Containing an Anionic Surfactant. *Synth. Met.* **1998**, *98* (1), 65–70. https://doi.org/10.1016/S0379-6779(98)00148-9.

(32) Zozoulenko, I.; Singh, A.; Singh, S. K.; Gueskine, V.; Crispin, X.; Berggren, M. Polarons, Bipolarons, And Absorption Spectroscopy of PEDOT. *ACS Appl. Polym. Mater.* **2019**, *1* (1), 83–94. https://doi.org/10.1021/acsapm.8b00061.

(33) Carli, S.; Trapella, C.; Armirotti, A.; Fantinati, A.; Ottonello, G.; Scarpellini, A.; Prato, M.; Fadiga, L.; Ricci, D. Biochemically Controlled Release of Dexamethasone Covalently Bound to PEDOT. *Chem. - A Eur. J.* **2018**, *24* (41), 10300–10305. https://doi.org/10.1002/chem.201801499.

(34) Zotti, G.; Zecchin, S.; Schiavon, G.; Louwet, F.; Groenendaal, L.; Crispin, X.; Osikowicz, W.; Salaneck, W.; Fahlman, M. Electrochemical and XPS Studies toward the Role of Monomeric and Polymeric Sulfonate Counterions in the Synthesis, Composition, and Properties of Poly(3,4-Ethylenedioxythiophene). *Macromolecules* **2003**, *36* (9), 3337–3344. https://doi.org/10.1021/ma021715k.

(35) Håkansson, A.; Han, S.; Wang, S.; Lu, J.; Braun, S.; Fahlman, M.; Berggren, M.; Crispin, X.; Fabiano, S. Effect of (3-Glycidyloxypropyl)Trimethoxysilane (GOPS) on the Electrical Properties of PEDOT:PSS Films. *J. Polym. Sci. Part B Polym. Phys.* **2017**, *55* (10), 814–820. https://doi.org/10.1002/polb.24331.

(36) Gangopadhyay, R.; Das, B.; Molla, M. R. How Does PEDOT Combine with PSS? Insights from Structural Studies. *RSC Adv.* **2014**, *4* (83), 43912–43920. https://doi.org/10.1039/c4ra08666j.

(37) Szentirmay, M. N.; Campbell, L. F.; Martin, C. R. Silane Coupling Agents for Attaching Nafion to Glass and Silica. *Anal. Chem.* **1986**, *58* (3), 661–662. https://doi.org/10.1021/ac00294a042.

(38) Groenendaal, L.; Zotti, G.; Aubert, P. H.; Waybright, S. M.; Reynolds, J. R. Electrochemistry of Poly(3,4-Alkylenedioxythiophene) Derivatives. *Adv. Mater.* **2003**, *15* (11), 855–879. https://doi.org/10.1002/adma.200300376.

(39) Gruger, A.; André, R.; Schmatko, T.; Colomban, P. Nanostructure of Nafion® Membranes at Different States of Hydration: An IR and Raman Study. *Vib. Spectrosc.* **2001**, *26* (2), 215–225. https://doi.org/10.1016/S0924-2031(01)00116-3.

(40) Tsai, C. E.; Hwang, B. J. Intermolecular Interactions between Methanol/Water Molecules and Nafion™ Membrane: An Infrared Spectroscopy Study. *Fuel Cells* **2007**, *7* (5), 408–416. https://doi.org/10.1002/fuce.200700002.

(41) Choi, J. W.; Han, M. G.; Kim, S. Y.; Oh, S. G.; Im, S. S. Poly(3,4-Ethylenedioxythiophene) Nanoparticles Prepared in Aqueous DBSA Solutions. *Synth. Met.* **2004**, *141* (3), 293–299. https://doi.org/10.1016/S0379-6779(03)00419-3.

(42) Kvarnström, C.; Neugebauer, H.; Blomquist, S.; Ahonen, H. J.; Kankare, J.; Ivaska, A. In Situ Spectroelectrochemical Characterization of Poly(3,4-Ethylenedioxythiophene). *Electrochim. Acta* **1999**, *44* (16), 2739–2750. https://doi.org/10.1016/S0013-4686(98)00405-8.

(43) Greczynski, G.; Kugler, T.; Salaneck, W. R. Characterization of the PEDOT-PSS System by Means of X-Ray and Ultraviolet Photoelectron Spectroscopy. *Thin Solid Films* **1999**, *354* (1), 129–135. https://doi.org/10.1016/S0040-6090(99)00422-8.

(44) Greczynski, G.; Kugler, T.; Keil, M.; Osikowicz, W.; Fahlman, M.; Salaneck, W. R. Photoelectron Spectroscopy of Thin Films of PEDOT-PSS Conjugated Polymer Blend: A Mini-Review and Some New Results. *J. Electron Spectros. Relat. Phenomena* **2001**, *121* (1–3), 1–17. https://doi.org/10.1016/S0368-2048(01)00323-1.

(45) Carli, S.; Lambertini, L.; Zucchini, E.; Ciarpella, F.; Scarpellini, A.; Prato, M.; Castagnola, E.; Fadiga, L.; Ricci, D. Single Walled Carbon Nanohorns Composite for Neural Sensing and Stimulation. *Sensors Actuators, B Chem.* **2018**, *271* (May),

280–288. https://doi.org/10.1016/j.snb.2018.05.083.

(46) Dickhaus, B. N.; Priefer, R. Determination of Polyelectrolyte PKa Values Using Surface-to-Air Tension Measurements. *Colloids Surfaces A Physicochem. Eng. Asp.* **2016**, *488* (5 January), 15–19. https://doi.org/10.1016/j.colsurfa.2015.10.015.

(47) Ma, C.; Zhang, L.; Mukerjee, S.; Ofer, D.; Nair, B. An Investigation of Proton Conduction in Select PEM's and Reaction Layer Interfaces-Designed for Elevated Temperature Operation. *J. Memb. Sci.* **2003**, *219* (1–2), 123–136. https://doi.org/10.1016/S0376-7388(03)00194-7.

(48) Friedman, A. K.; Shi, W.; Losovyj, Y.; Siedle, A. R.; Baker, L. A. Mapping Microscale Chemical Heterogeneity in Nafion Membranes with X-Ray Photoelectron Spectroscopy a B. *J. Electrochem. Soc.* **2018**, *165* (11), H733–H741. https://doi.org/10.1149/2.0771811jes.

(49) Spanninga, S. A.; Martin, D. C.; Chen, Z. X-Ray Photoelectron Spectroscopy Study of Counterion Incorporation in Poly(3,4-Ethylenedioxythiophene). *J. Phys. Chem.*

C **2009**, *113* (14), 5585–5592. https://doi.org/10.1021/jp811282f.

(50) Susac, D.; Kono, M.; Wong, K. C.; Mitchell, K. A. R. XPS Study of Interfaces in a Two-Layer Light-Emitting Diode Made from PPV and Nafion with Ionically Exchanged Ru(Bpy) 32+. *Appl. Surf. Sci.* **2001**, *174* (1), 43–50. https://doi.org/10.1016/S0169-4332(01)00026-5.

(51) Hsu, W. Y.; Gierke, T. D. Ion Transport and Clustering in Nafion Perfluorinated Membranes. *J. Memb. Sci.* **1983**, *13* (3), 307–326. https://doi.org/10.1016/S0376-7388(00)81563-X.

(52) Im, S. G.; Gleason, K. K. Systematic Control of the Electrical Conductivity of Poly(3,4- Ethylenedioxythiophene) via Oxidative Chemical Vapor Deposition. *Macromolecules* **2007**, *40* (18), 6552–6556. https://doi.org/10.1021/ma0628477.

(53) Dkhissi, A.; Beljonne, D.; Lazzaroni, R.; Louwet, F.; Groenendaal, L.; Brédas, J. L. Density Functional Theory and Hartree-Fock Studies of the Geometric and Electronic Structure of Neutral and Doped Ethylenedioxythiophene (EDOT)

Oligomers. *Int. J. Quantum Chem.* **2003**, *91* (3), 517–523. https://doi.org/10.1002/qua.10446.

(54) Heeger, A. J. Charge Storage in Conducting Polymers: Solitons, Polarons, and Bipolarons. *Polym. J.* **1985**, *17* (1), 201–208. https://doi.org/10.1295/polymj.17.201.

(55) Ouyang, J.; Xu, Q.; Chu, C. W.; Yang, Y.; Li, G.; Shinar, J. On the Mechanism of Conductivity Enhancement in Poly(3,4- Ethylenedioxythiophene):Poly(Styrene Sulfonate) Film through Solvent Treatment. *Polymer (Guildf).* **2004**, *45* (25), 8443–8450. https://doi.org/10.1016/j.polymer.2004.10.001.

(56) Marzocchi, M.; Gualandi, I.; Calienni, M.; Zironi, I.; Scavetta, E.; Castellani, G.; Fraboni, B. Physical and Electrochemical Properties of PEDOT:PSS as a Tool for Controlling Cell Growth. *ACS Appl. Mater. Interfaces* **2015**, *7* (32), 17993–18003. https://doi.org/10.1021/acsami.5b04768.

(57) Xia, Y.; Ouyang, J. Significant Different Conductivities of the Two Grades of Poly(3,4-Ethylenedioxythiophene):Poly(Styrenesulfonate), Clevios P and Clevios

PH1000, Arising from Different Molecular Weights. *ACS Appl. Mater. Interfaces* **2012**, *4* (8), 4131–4140. https://doi.org/10.1021/am300881m.

(58) Danielsson, P.; Bobacka, J.; Ivaska, A. Electrochemical Synthesis and Characterization of Poly(3,4- Ethylenedioxythiophene) in Ionic Liquids with Bulky Organic Anions. *J. Solid State Electrochem.* **2004**, *8* (10), 809–817. https://doi.org/10.1007/s10008-004-0549-2.

(59) Barsoukov, E.; Macdonald, J. R. *Impedance Spectroscopy: Theory, Experiment, and Applications*; John Wiley & Sons, Inc., 2005. https://doi.org/10.1002/0471716243.

(60) Castagnola, E.; Carli, S.; Vomero, M.; Scarpellini, A.; Prato, M.; Goshi, N.; Fadiga, L.; Kassegne, S.; Ricci, D. Multilayer Poly(3,4-Ethylenedioxythiophene)-Dexamethasone and Poly(3,4-Ethylenedioxythiophene)-Polystyrene Sulfonate-Carbon Nanotubes Coatings on Glassy Carbon Microelectrode Arrays for Controlled Drug Release. *Biointerphases* **2017**, *12* (3), 031002. https://doi.org/10.1116/1.4993140.

(61) Ren, X.; Pickup, P. G. Ion Transport in Polypyrrole and a Polypyrrole/Polyanion Composite. *J. Phys. Chem.* **1993**, *97* (20), 5356–5362. https://doi.org/10.1021/j100122a029.

(62) Bobacka, J.; Lewenstam, A.; Ivaska, A. Electrochemical Impedance Spectroscopy of Oxidized Poly(3,4-Ethylenedioxythiophene) Film Electrodes in Aqueous Solutions. *J. Electroanal. Chem.* **2000**, *489* (1), 17–27. https://doi.org/10.1016/S0022-0728(00)00206-0.

(63) Reza, K. M.; Gurung, A.; Bahrami, B.; Mabrouk, S.; Elbohy, H.; Pathak, R.; Chen, K.; Chowdhury, A. H.; Rahman, M. T.; Letourneau, S.; Yang, H. C.; Saianand, G.; Elam, J. W.; Darling, S. B.; Qiao, Q. Tailored PEDOT:PSS Hole Transport Layer for Higher Performance in Perovskite Solar Cells: Enhancement of Electrical and Optical Properties with Improved Morphology. *J. Energy Chem.* **2020**, *44* (May 2020), 41–50. https://doi.org/10.1016/j.jechem.2019.09.014.

(64) Khodagholy, D.; Rivnay, J.; Sessolo, M.; Gurfinkel, M.; Leleux, P.; Jimison, L. H.; Stavrinidou, E.; Herve, T.; Sanaur, S.; Owens, R. M.; Malliaras, G. G. High

Transconductance Organic Electrochemical Transistors. *Nat. Commun.* **2013**, *4*, 1–6. https://doi.org/10.1038/ncomms3133.

(65) Di Lauro, M.; la Gatta, S.; Bortolotti, C. A.; Beni, V.; Parkula, V.; Drakopoulou, S.; Giordani, M.; Berto, M.; Milano, F.; Cramer, T.; Murgia, M.; Agostiano, A.; Farinola, G. M.; Trotta, M.; Biscarini, F. A Bacterial Photosynthetic Enzymatic Unit Modulating Organic Transistors with Light. *Adv. Electron. Mater.* **2019**, *6* (1), 1900888. https://doi.org/10.1002/aelm.201900888.

(66) Elschner, A.; Kirchmeyer, S.; Lovenich, W.; Merker, U.; Reuter, K. *PEDOT: Principles and Applications of an Intrinsically Conductive Polymer*; CRC Press, 2010.

(67) Van De Burgt, Y.; Lubberman, E.; Fuller, E. J.; Keene, S. T.; Faria, G. C.; Agarwal, S.; Marinella, M. J.; Alec Talin, A.; Salleo, A. A Non-Volatile Organic Electrochemical Device as a Low-Voltage Artificial Synapse for Neuromorphic Computing. *Nat. Mater.* **2017**, *16* (4), 414–418. https://doi.org/10.1038/NMAT4856.

(68) Di Lauro, M.; Berto, M.; Giordani, M.; Benaglia, S.; Schweicher, G.; Vuillaume, D.; Bortolotti, C. A.; Geerts, Y. H.; Biscarini, F. Liquid-Gated Organic Electronic Devices Based on High-Performance Solution-Processed Molecular Semiconductor. *Adv. Electron. Mater.* **2017**, *3* (9), 1–6. https://doi.org/10.1002/aelm.201700159.

(69) Martin, S. J.; Grimwood, P. D.; Morris, R. G. M. Synaptic Plasticity and Memory: An Evaluation of the Hypothesis. *Annu. Rev. Neurosci.* **2000**, *23* (1), 649–711. https://doi.org/10.1146/annurev.neuro.23.1.649.

(70) Burgt, Y. Van De; Melianas, A.; Keene, S. T.; Malliaras, G.; Salleo, A. Organic Electronics for Neuromorphic Computing. *Nat. Electron.* **2018**, *1*, 386–397. https://doi.org/10.1038/s41928-018-0103-3.

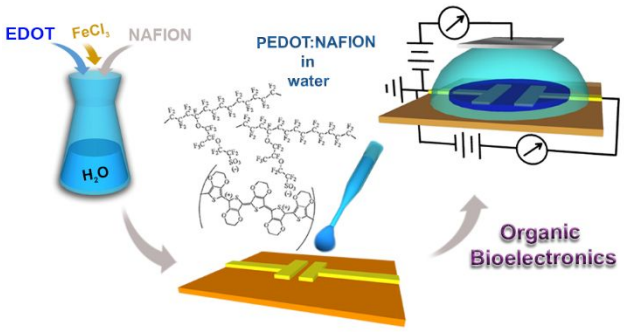

Table of Contents